The 2024–2025 seismic sequence in the Santorini-Amorgos region: Insights into volcano-tectonic activity through high-resolution seismic monitoring

Ioannis Fountoulakis[1], Christos P. Evangelidis[1]

[1]Institute of Geodynamics, National Observatory of Athens, Greece

Contents of this file

April 18, 2025, 9:28am

Text S1. Data Availability Although the study area is surrounded by scattered islands, the availability of seismic stations and data was initially suboptimal due to a lack of long term funding for maintaining permanent infrastructure. Most nearby stations were located on Santorini island, resulting in a significant azimuthal gap that reduces the accuracy of location solutions. The seismic network was later enhanced with the addition of stations HT.ANYD, HL.AMGA, HL.ANAF, HL.ASTA and HA.IOSI across several nearby islands (Fig. 1). The installation of station ANYD (03/02/2025) on a small, remote, inhabited island (Anydros) was a decisive improvement, as it is located close to the center of the current seismic activity. Its proximity to the active area significantly improves event detection and location accuracy. A detailed overview of stations position and data availability is presented in Figure S1.

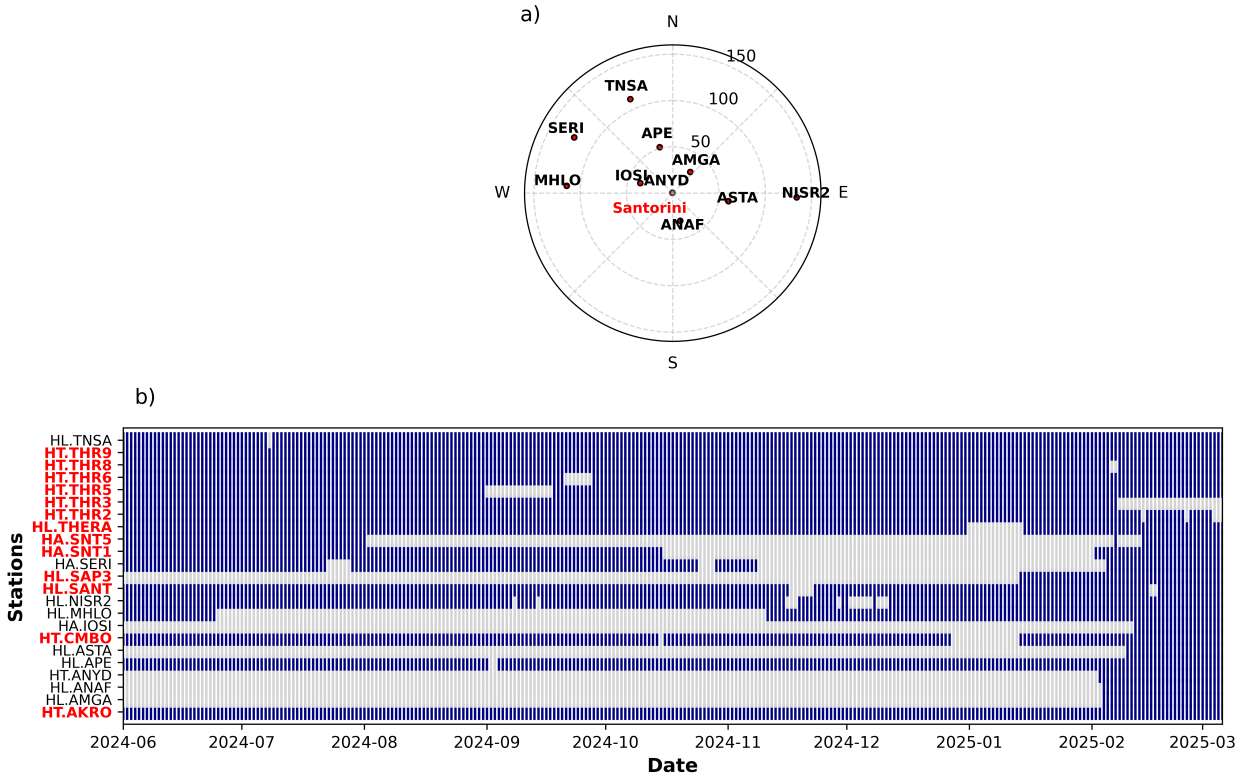

Figure S1. Data distribution and availability. (a) Spatial distribution of seismic stations used in this study centered on Anydros Island. (b) Data availability of seismic stations from June 2024 to March 2025. Blue segments indicate periods of data availability, while gray segments represent gaps in data recording. Stations labeled in red are located on Santorini Island.

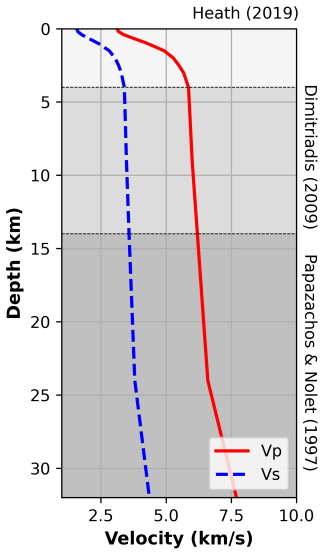

Figure S2. Local velocity model.

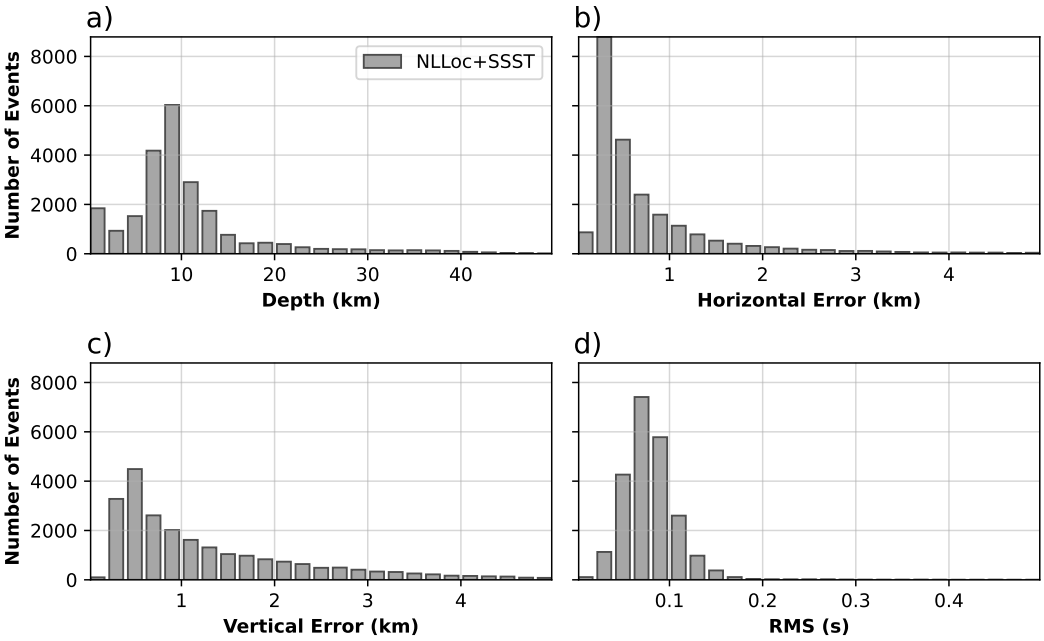

Figure S3. Distribution of (a) depth, (b) horizontal error, (c) vertical error and d) rms values after the absolute relocation (with NLLoc and SSST).

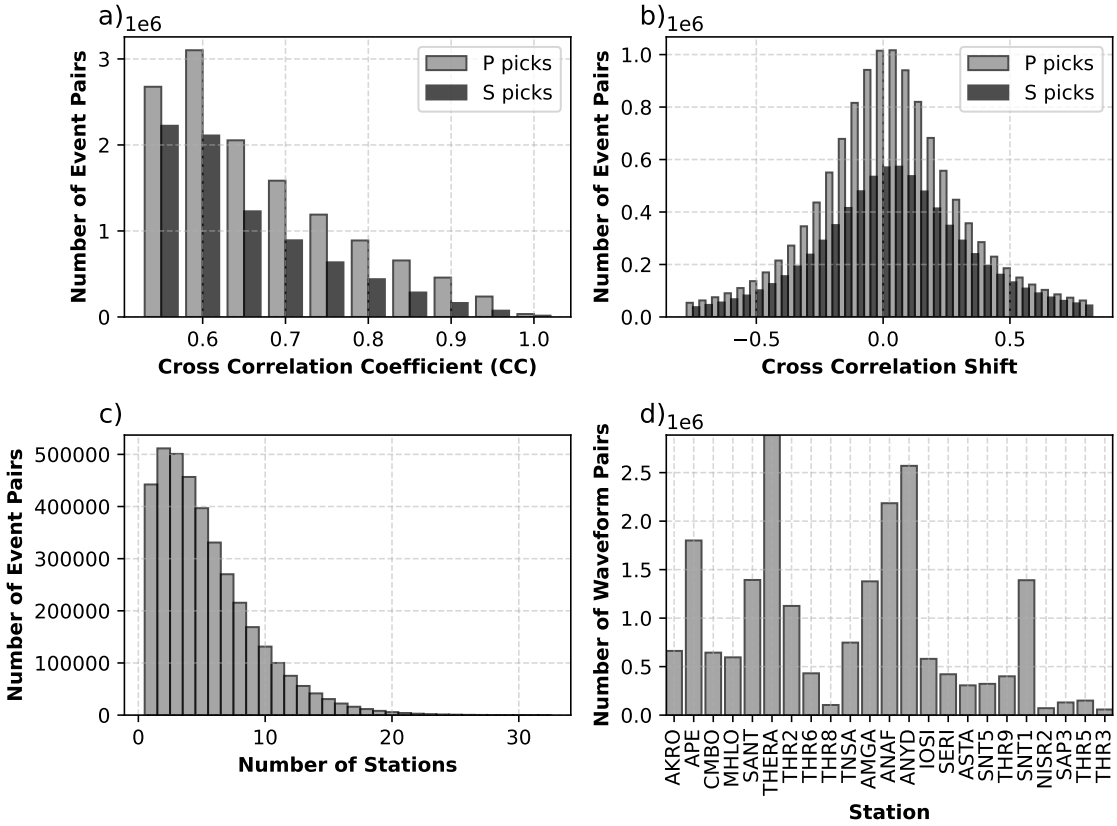

Figure S4. Histograms based on the CC results with (a) the number of event pairs at different CC for P and S picks, (b) the CC shift values, (c) the number of stations distribution of the event pairs and (d) the number of waveform pairs with CC higher than 0.50 at the used stations.

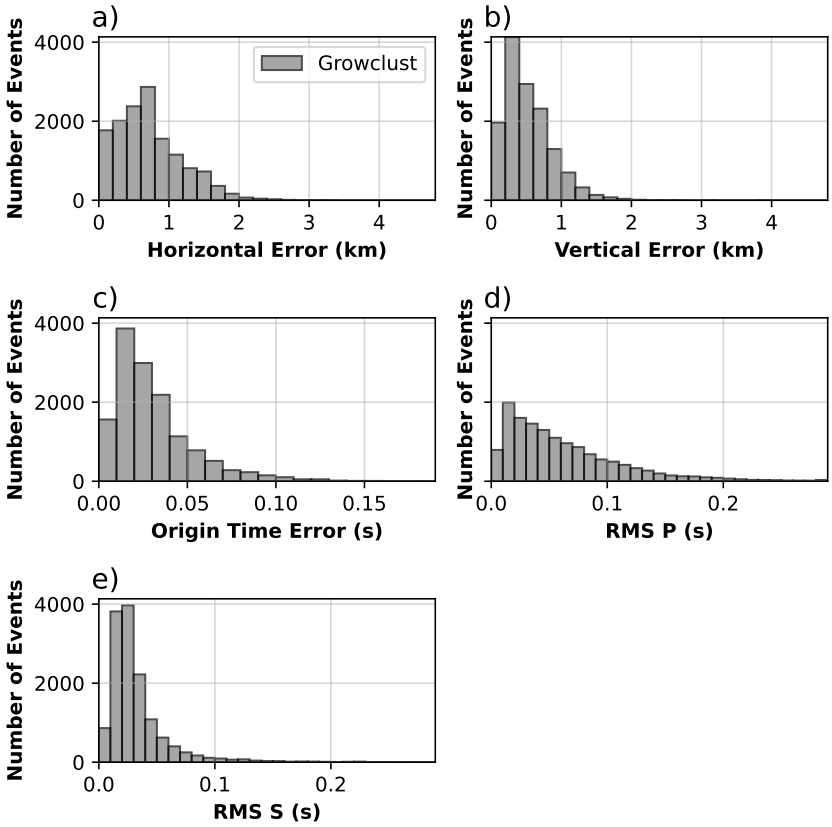

Figure S5. Error statistics of the relative relocation including the (a) horizontal error, (b) the vertical error, (c) the origin time error, the P (d) and S (e) rms.

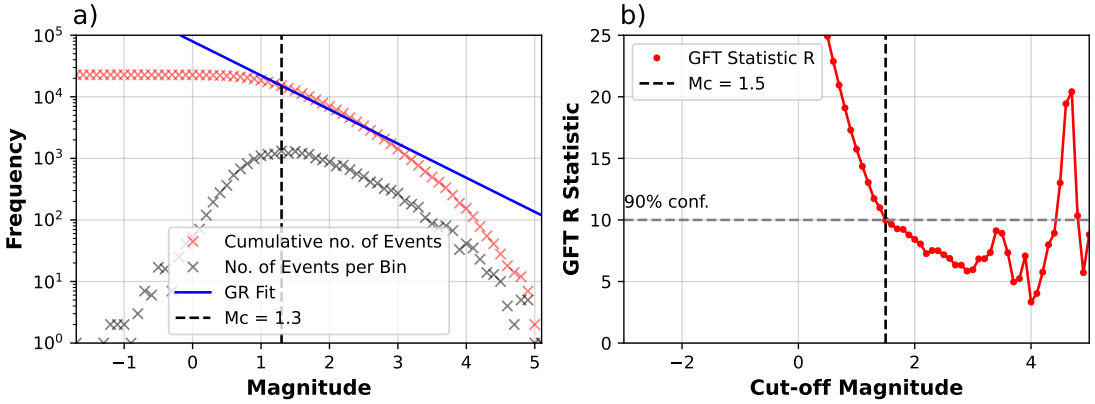

Figure S6. Magnitude of completeness following the (a) maximum curvature and (b) the goodness-of-fit (GFT) method (Wiemer & Wyss, 2000).

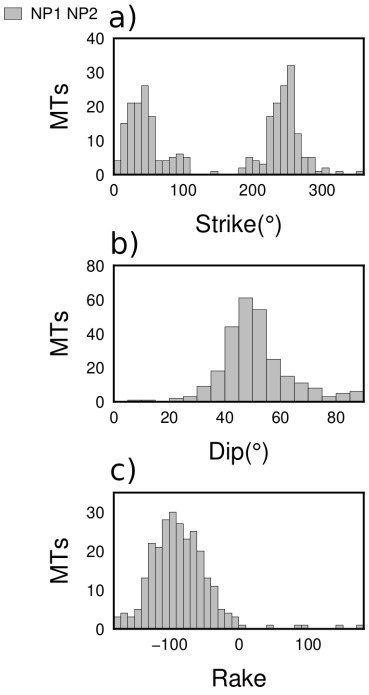

Figure S7. Distribution of MTs: (a) strike, (b) dip and (c) rake for both of the determined planes.

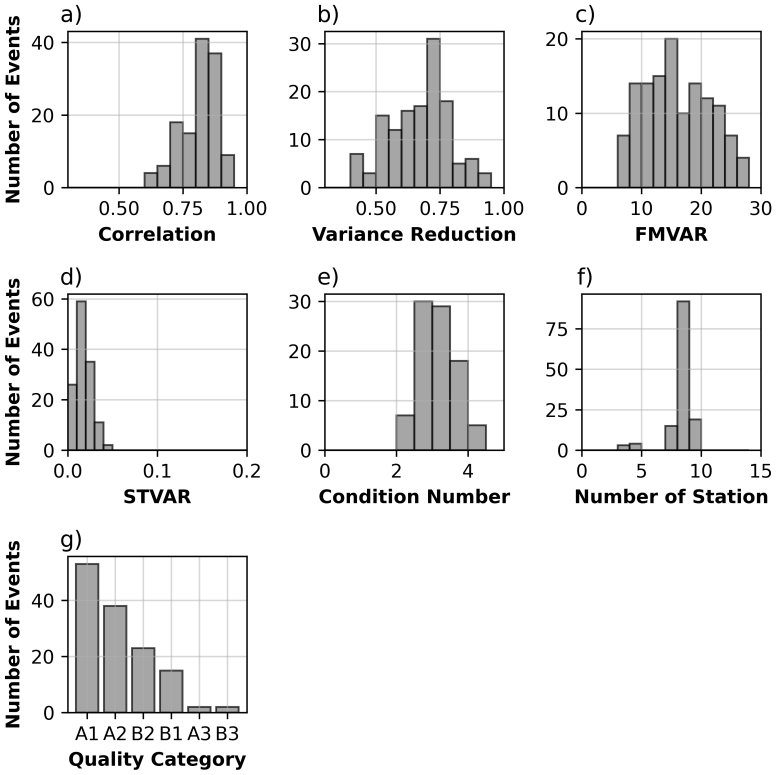

Figure S8. Distribution of MTs quality parameters: (a) correlation values, (b) variance reduction, (c) FMWAR, (d) STVAR, (e) condition number, (f) number of stations used, and (g) quality category classification of events (Scognamiglio et al., 2009).

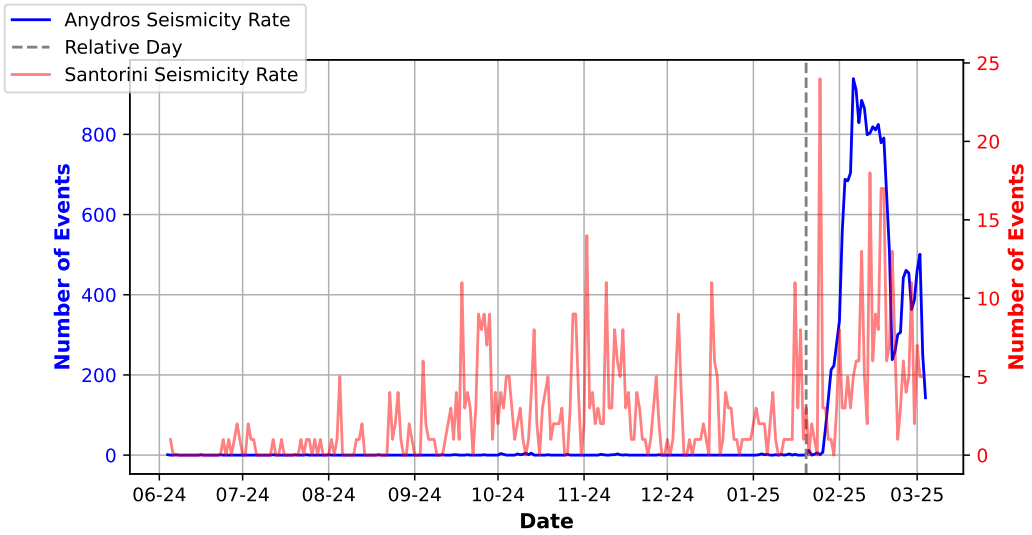

Figure S9. Daily seismicity rate for the relocated earthquake catalog during the study period, separated into events within the boundaries of Santorini Island and those offshore (Anydros activity). The gray dashed line indicates the start time of the reference day adopted in Figure 1.

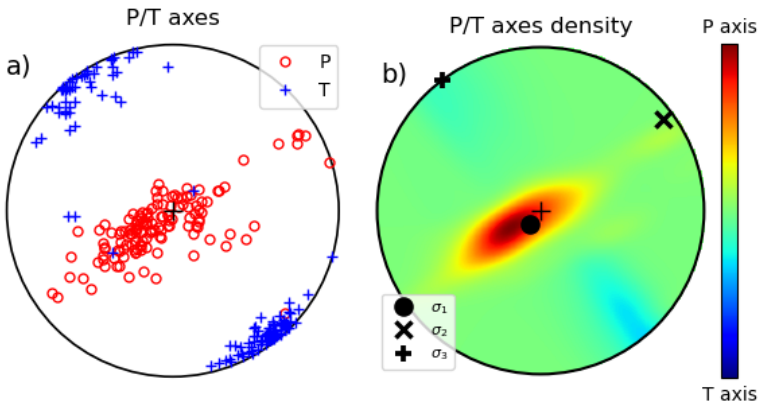

Figure S10. Distribution and density of P and T Axes from focal mechanism solutions: (a) stereographic projection of P (pressure) and T (tension) axes, where red circles represent P axes and blue crosses represent T axes. (b) Density plot of the P/T axis distribution, with a color scale indicating density variations. The principal stress axes ($\sigma_1, \sigma_2, \sigma_3$) are also shown.

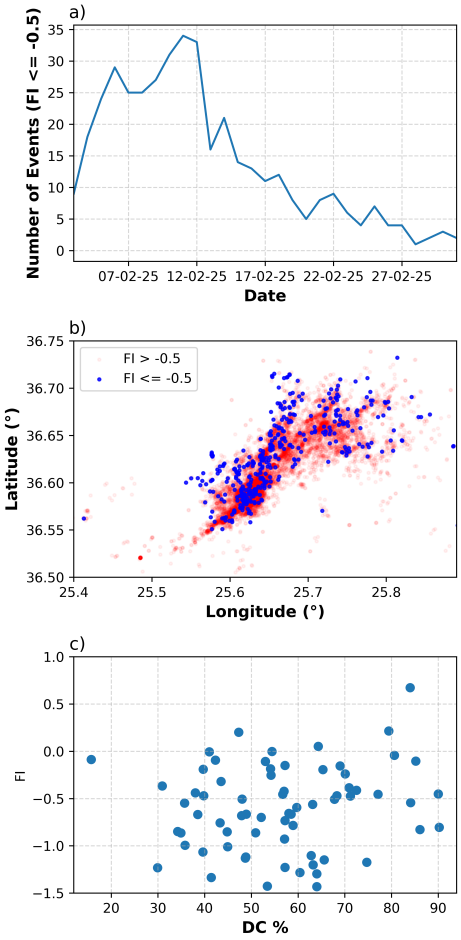

Figure S11. FI analysis: (a) Temporal distribution of seismic events with low FI (FI $\leq$ –0.5), (b) Spatial distribution of events categorized by FI values. Events with FI $\leq$ –0.5 (blue) are compared to those with FI $>$ –0.5 (red), and (c) scatter plot of FI versus double-couple percentage.

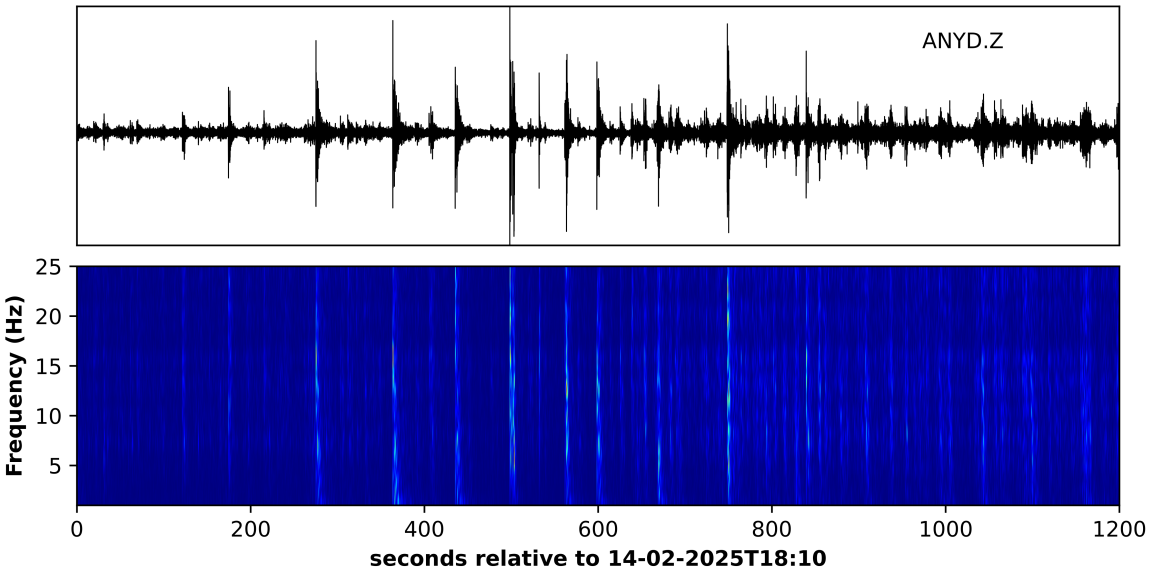

Figure S12. Example of observed series of high-frequency bursts.

References

Scognamiglio, L., Tinti, E., & Michelini, A. (2009). Real-time determination of seismic moment tensor for the italian region. *Bulletin of the Seismological Society of America*, *99*(4), 2223-2242. doi: 10.1785/0120080104

Wiemer, S., & Wyss, M. (2000). Minimum magnitude of completeness in earthquake catalogs: Examples from alaska, the western united states, and japan. *Bulletin of the Seismological Society of America*, *90*, 859–869. doi: 10.1785/0119990114